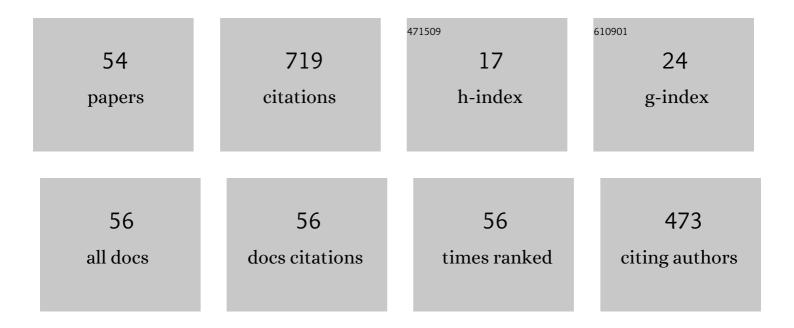
## Bo Song

## List of Publications by Year in descending order

Source: https://exaly.com/author-pdf/4794193/publications.pdf Version: 2024-02-01



RO SONC

#	Article	IF	CITATIONS
1	Effects of vanadium precipitates on hydrogen trapping efficiency and hydrogen induced cracking resistance in X80 pipeline steel. International Journal of Hydrogen Energy, 2018, 43, 17353-17363.	7.1	58
2	Large enhancement of energy-storage properties of compositional graded (Pb1â^'xLax)(Zr0.65Ti0.35)O3 relaxor ferroelectric thick films. Applied Physics Letters, 2013, 103, .	3.3	46
3	Intragranular Ferrite Formation Mechanism and Mechanical Properties of Non-quenched-and-tempered Medium Carbon Steels. Steel Research International, 2008, 79, 390-395.	1.8	41
4	Effect of vanadium content on hydrogen diffusion behaviors and hydrogen induced ductility loss of X80 pipeline steel. Materials Science & Engineering A: Structural Materials: Properties, Microstructure and Processing, 2019, 742, 712-721.	5.6	40
5	Role of Lanthanum Addition on Acicular Ferrite Transformation in C–Mn Steel. ISIJ International, 2017, 57, 1261-1267.	1.4	38
6	Separating Behavior of Nonmetallic Inclusions in Molten Aluminum Under Super-Gravity Field. Metallurgical and Materials Transactions B: Process Metallurgy and Materials Processing Science, 2015, 46, 2190-2197.	2.1	34
7	Formation of Acicular Ferrite in Mg Treated Ti-bearing C–Mn Steel. ISIJ International, 2015, 55, 1468-1473.	1.4	32
8	The Refining Mechanism of Super Gravity on the Solidification Structure of Al-Cu Alloys. Materials, 2016, 9, 1001.	2.9	30
9	Effect of Cerium on Characteristic of Inclusions and Grain Boundary Segregation of Arsenic in Iron Melts. Steel Research International, 2015, 86, 1430-1438.	1.8	29
10	Dielectric properties and energy-storage performances of (1Ââ~'Âx)Pb(Mg1/3Nb2/3)O3–xPbTiO3 relaxor ferroelectric thin films. Journal of Materials Science: Materials in Electronics, 2015, 26, 9583-9590.	2.2	27
11	Influence of Ce on Characteristics of Inclusions and Microstructure of Pure Iron. Journal of Iron and Steel Research International, 2011, 18, 38-44.	2.8	22
12	Enriching and Separating Primary Copper Impurity from Pb-3 Mass Pct Cu Melt by Super-Gravity Technology. Metallurgical and Materials Transactions B: Process Metallurgy and Materials Processing Science, 2016, 47, 2714-2724.	2.1	22
13	Effect of Super-gravity Field on Grain Refinement and Tensile Properties of Cu–Sn Alloys. ISIJ International, 2018, 58, 98-106.	1.4	22
14	Removal of Inclusions from Molten Aluminum by Supergravity Filtration. Metallurgical and Materials Transactions B: Process Metallurgy and Materials Processing Science, 2016, 47, 3435-3445.	2.1	21
15	Effect of Mg on the Evolution of Inclusions and Formation of Acicular Ferrite in La–Tiâ€Treated Steels. Steel Research International, 2020, 91, 1900563.	1.8	19
16	Effects of Mg and La on the evolution of inclusions and microstructure in Ca-Ti treated steel. International Journal of Minerals, Metallurgy and Materials, 2021, 28, 1940-1948.	4.9	19
17	Effect of austenitizing temperature on microstructure in 16Mn steel treated by cerium. International Journal of Minerals, Metallurgy and Materials, 2011, 18, 652-658.	4.9	18
18	Effect of Ti–Mg Treatment on the Impact Toughness of Heat Affected Zone in 0.15%C–1.31%Mn Steel. Steel Research International, 2018, 89, 1700355.	1.8	16

Bo Song

#	Article	IF	CITATIONS
19	Effect of Arsenic and Copper+Arsenic on High Temperature Oxidation and Hot Shortness Behavior of C–Mn Steel. ISIJ International, 2016, 56, 1232-1240.	1.4	14
20	Effect of Cerium Content on the Evolution of Inclusions and Formation of Acicular Ferrite in Ti-Mg-Killed EH36 Steel. Metals, 2020, 10, 863.	2.3	12
21	Effect of arsenic content and quenching temperature on solidification microstructure and arsenic distribution in iron-arsenic alloys. International Journal of Minerals, Metallurgy and Materials, 2015, 22, 704-713.	4.9	11
22	Effects of CeO <sub>2</sub> on Melting Temperature, Viscosity, and Structure of CaF <sub>2</sub> -bearing and B <sub>2</sub> 0 <sub>3</sub> -containing Mold Fluxes for Casting Rare Earth Alloy Heavy Rail Steels. ISIJ International, 2019, 59, 1242-1249.	1.4	11
23	Effects of finish rolling deformation on hydrogen-induced cracking and hydrogen-induced ductility loss of high-vanadium TMCP X80 pipeline steel. International Journal of Hydrogen Energy, 2020, 45, 30828-30844.	7.1	10
24	Effect of heat input on microstructure and toughness of rare earth-contained C–Mn steel. Journal of Iron and Steel Research International, 2018, 25, 1033-1042.	2.8	9
25	Effect of CeO2 on heat transfer and crystallization behavior of rare earth alloy steel mold fluxes. International Journal of Minerals, Metallurgy and Materials, 2019, 26, 565-572.	4.9	8
26	Effect of manganese sulfide on the precipitation behavior of tin in steel. International Journal of Minerals, Metallurgy and Materials, 2014, 21, 654-659.	4.9	7
27	Effects of Mn and Al on the Intragranular Acicular Ferrite Formation in Rare Earth Treated C–Mn Steel. High Temperature Materials and Processes, 2017, 36, 683-691.	1.4	7
28	Synthesis and densification of zirconium diboride prepared by carbothermal reduction. Rare Metals, 2018, 37, 1076-1081.	7.1	7
29	Effect of Tempering Temperature after Thermo-Mechanical Control Process on Microstructure Characteristics and Hydrogen-Induced Ductility Loss in High-Vanadium X80 Pipeline Steel. Materials, 2020, 13, 2839.	2.9	7
30	Designing cross-region ecological compensation scheme by integrating habitat maintenance services production and consumption—A case study of Jing-Jin-Ji region. Journal of Environmental Management, 2022, 311, 114820.	7.8	7
31	Separation of Non-metallic Inclusions from a Fe-Al-O Melt Using a Super-Gravity Field. Metallurgical and Materials Transactions B: Process Metallurgy and Materials Processing Science, 2018, 49, 34-44.	2.1	6
32	Macrosegregation behavior of solute Cu in the solidifying Al-Cu alloys in super-gravity field. Metallurgical Research and Technology, 2018, 115, 506.	0.7	6
33	The Microstructure and Property of the Heat Affected zone in C-Mn Steel Treated by Rare Earth. High Temperature Materials and Processes, 2019, 38, 362-369.	1.4	6
34	A Mathematical Model of COREX Process with Top Gas Recycling. Steel Research International, 2021, 92, 2000292.	1.8	6
35	Effect of Rare Earth Ce on Modifying Inclusions in Al-killed X80 Pipeline Steel. Transactions of the Indian Institute of Metals, 2022, 75, 2837-2846.	1.5	6
36	Electrochemical reduction behavior of Hf(IV) in molten NaCl–KCl–K2HfCl6 system. Rare Metals, 2016, 35, 655-660.	7.1	5

Bo Song

#	Article	IF	CITATIONS
37	Effects of cooling processes on microstructure and susceptibility of hydrogenâ€induced cracking of X80 pipeline steel. Materials and Corrosion - Werkstoffe Und Korrosion, 2018, 69, 590-600.	1.5	5
38	Multi-Objective Optimization of Cost Saving and Emission Reduction in Blast Furnace Ironmaking Process. Metals, 2018, 8, 979.	2.3	5
39	Reliability analysis of wind turbines under nonâ€Gaussian wind load. Structural Design of Tall and Special Buildings, 2018, 27, e1443.	1.9	4
40	Microstructure and physical properties of a mullite brick in blast furnace hearth: influence of temperature. Ironmaking and Steelmaking, 2020, , 1-7.	2.1	4
41	Influence of temperature on the microstructure and physical properties of corundum refractory brick in the blast furnace hearth. Ironmaking and Steelmaking, 2020, 47, 263-270.	2.1	3
42	Evolution of inclusions in Mg-RE-Ti treated steels with different Al contents and their influence on acicular ferrite. Metallurgical Research and Technology, 2021, 118, 208.	0.7	3
43	Effect of Ca on the evolution of inclusions and the formation of acicular ferrite in Ti–Mg killed EH36 steel. Ironmaking and Steelmaking, 2021, 48, 1115-1122.	2.1	3
44	Influence of top gas recycling technology on operation parameters and CO2 emission of COREX process. Ironmaking and Steelmaking, 2021, 48, 693-702.	2.1	2
45	Effect of Mg, La and Ca addition order on inclusions and microstructure of Ti-bearing C–Mn steel. Ironmaking and Steelmaking, 2022, 49, 189-198.	2.1	2
46	Effect of Al and S on the Evolution of Inclusion and Formation of Acicular Ferrite in the Mg-RE-Ti-Treated Steel. Transactions of the Indian Institute of Metals, 2022, 75, 2221-2230.	1.5	2
47	In Situ Observation of the Evolution of Intragranular Acicular Ferrite at Mg-containing Inclusions in 16Mn Steel. Journal for Manufacturing Science and Production, 2013, 13, .	0.1	1
48	Effect of Manganese Sulphide Size on the Precipitation of Tin Heterogeneous Nucleation in as-Cast Steel. High Temperature Materials and Processes, 2015, 34, .	1.4	1
49	Influence of Tempering Treatment on Precipitation Behavior, Microstructure, Dislocation Density and Hydrogen-Induced Ductility Loss in High-Vanadium Hot-Rolled X80 Pipeline Steel. Minerals, Metals and Materials Series, 2019, , 1111-1122.	0.4	1
50	Effect of Vanadium and Titanium on Desulfurization of CaO Slag in Liquid Iron. Metals, 2019, 9, 1239.	2.3	1
51	The Interaction Force between Scheelite and Scheelite/Fluorite/Calcite Measured Using Atomic Force Microscopy. Journal of Chemistry, 2020, 2020, 1-15.	1.9	1
52	Evolution of Inclusions and Microstructure in Ca‣aâ€Treated Câ€Mn Steel with Different Mg Contents. Steel Research International, 0, , 2200319.	1.8	1
53	Effect of Super Gravity on the Solidification Structure and C Segregation of High-Carbon Steel. Minerals, Metals and Materials Series, 2017, , 571-579.	0.4	0
54	Directional separation of nonmetallic inclusions from copper melt reinforced by supergravity. Metallurgical Research and Technology, 2022, 119, 307.	0.7	0